Urea Delays High-Temperature Crosslinking of Polyacrylamide for in Situ Preparation of an Organic/Inorganic Composite Gel

Li Liang , Junlong Li , Dongxiang Li * , Jie Xu , Bin Zheng , Jikuan Zhao *

Posted Date: 20 February 2025

doi: 10.20944/preprints202502.1604.v1

Keywords: polyacrylamide; crosslinking reaction; composite gel; urea; delayed gelation; in situ preparation

 doi:10.20944/preprints202502.1604.v1

Article

Urea Delays High-Temperature Crosslinking of Polyacrylamide for in Situ Preparation of an Organic/Inorganic Composite Gel

Li Liang [1,2], Junlong Li [1,2], Dongxiang Li [1,2,*], Jie Xu [1,2], Bin Zheng [1,2] and Jikuan Zhao [1,2,*]

[1] Key Laboratory of Optic-electro Sensing and Analytical Chemistry of Life Science (Ministry of Education) , Qingdao University of Science and Technology, Qingdao 266042, China

[2] Lab of Colloids and Functional Nanostructures, College of Chemistry and Molecular Engineering, Qingdao University of Science and Technology, Qingdao 266042, China

* Correspondence: lidx@qust.edu.cn (D.L.); forestzhao@qust.edu.cn (J.Z.)

Abstract: To address the rapid crosslinking reaction and short stability duration of polyacrylamide gel under high salinity and temperature conditions, this paper proposes the use of urea to delay the nucleophilic substitution crosslinking reaction among polyacrylamide, hydroquinone, and formaldehyde. At the same time, urea also regulates the precipitation of calcium and magnesium ions, enabling the in situ preparation of an organic/inorganic composite gel of crosslinked polyacrylamide and carbonate particles. With calcium and magnesium ion concentrations at 6817 mg/L and total salinity at 15×10^4 mg/L, the gelation time can be controlled to range from 6.6 to 14.1 days at 95 °C and from 2.9 to 6.5 days at 120 °C. The corresponding composite gel can remain stable for up to 155 days and 135 days, respectively. The delayed gelation facilitates longer-distance diffusion of the gelling agent into the formation, and the enhancements in gel strength and stability provide a solid foundation for improving the effectiveness of profile control and water shut-off in oilfields. This innovative approach promotes the comprehensive utilization of mineral resources within the formation.

Keywords: polyacrylamide; crosslinking reaction; composite gel; urea; delayed gelation; in situ preparation

1. Introduction

The gelation time, stability duration, and mechanical strength of polymer gels are pivotal parameters for their successful application in oilfield profile control and water shut-off treatments [1–7]. These parameters directly influence the duration and effectiveness of on-site production operations. However, high temperatures can accelerate gelation, while high salinity conditions can drastically shorten the stability duration of polymer gels, presenting ongoing challenges for researchers [8–11]. Simply adjusting the concentrations of polymers and crosslinking agents has proven insufficient for effectively delaying gelation at elevated temperatures [12–15], with limited literature addressing the modulation of crosslinking reactions based on fundamental reaction mechanisms. To overcome these limitations and enhance gel performance, organic/inorganic composite gels (CG) have attracted significant attention [2,4,6,16–35]. The integration of organic and inorganic components within composite gels leverages various interactions including electrostatic forces, hydrogen bonding, and coordination bonds to markedly improve the strength and stability of the resulting materials [16–19]. A wide array of inorganic particles, including silica [16,19–22], titanium dioxide [23], alumina [24], zirconia [25], fly ash [26], Fe_3O_4 [27], montmorillonite [28–30], bentonite [31], laponite [17,32], magnesium aluminum layered double hydroxide [33], zirconium hydroxide [18], graphene oxide [23,34], micron graphite oxide powder [35], and carbon nanotubes [23], have been explored for this purpose. However, incorporating these inorganic particles often

 doi:10.20944/preprints202502.1604.v1

requires regulating particle size [19,20], layer thickness [28,30,33], and surface properties [29,31] to ensure compatibility. Some systems struggle with high-salinity formation waters, necessitating the use of low-concentration brines or freshwater for gel preparation [17,19,34], which limits practical applications. The in situ synthesis of organic/inorganic composite gels from high-salinity polymer solutions remains underexplored. It is well-known that multivalent metal ions such as Ca^{2+} and Mg^{2+} in formation brine can catalyze polymer hydrolysis, leading to over-crosslinking and syneresis at high temperature [18,36,37]. There is a need for scientific approaches to utilize mineral resources within formation for the effective in situ preparation of composite gels.

Significant research has explored the crosslinking reaction mechanisms involving polyacrylamide (PAM), hydrolyzed polyacrylamide (HPAM), binary and ternary copolymers containing acrylamide [1,4–7,12–15,38–43]. Organic crosslinkers that either contain or can produce formaldehyde are frequently utilized, including formaldehyde itself, hexamethylenetetramine (HMTA), phenol/catechol/resorcinol/hydroquinone (HQ)-formaldehyde or HMTA, and melamine-formaldehyde, etc [12–15,38–40,42–44]. The reaction mechanisms of these crosslinking systems typically fall into two categories [42]. The first involves hydroxymethylation reactions between formaldehyde and PAM or phenolic substances, leading to the introduction of hydroxymethyl groups on the amide nitrogen and ortho/para positions of phenolic hydroxyls, followed by condensation dehydration to form a three-dimensional network [1,4,43]. The second category encompasses hydroxymethylation reactions between formaldehyde and phenolic or melamine molecules, introducing hydroxymethyl groups that subsequently react with amine groups in the polymer's amide units through condensation, ultimately forming a robust three-dimensional gel structure [12–14,40].

HMTA, which gradually decomposes into formaldehyde and ammonia above 80 °C [14], has emerged as a more environmentally friendly alternative to formaldehyde. Studies [10,13,44] have examined the gelation performance of PAM/HMTA/HQ and HPAM/HMTA/methyl p-hydroxybenzoate crosslinking systems across varying pH levels. The reaction system can form a stable gel when the pH is maintained between 7.5 and 9.5. However, gelation does not occur when the pH exceeds 9.5 [10]. By lowering the pH of the reaction system from 7.9 to 4.5 using an acid solution, the gelation time is significantly reduced from 10.6 hours to 3.2 hours, and the gel strength increases from 0.053 MPa to 0.062 MPa [13]. It has been proposed that an acidic environment promotes the decomposition of HMTA into formaldehyde, which further accelerates the crosslinking reaction, leading to a faster reaction rate and increased crosslink density. In contrast, an alkaline environment inhibits the decomposition of HMTA and the subsequent crosslinking reactions [5,13]. Notably, in gel systems involving HMTA, the decomposition of HMTA generates ammonia gas, which reacts with water to dissociate and release hydroxide ions, thereby increasing the system's alkalinity. Consequently, when analyzing the impact of pH on gelation performance, the primary focus has been on how acidity and alkalinity influence the decomposition of HMTA, which is considered the main factor affecting the gelation performance of the reaction system. However, the direct effect of pH on the crosslinking reaction itself has often been overlooked.

Bryant et al. [15] investigated the gelation performance of acrylamide and the acrylamide-based AM-AMPS binary copolymer within a phenol-formaldehyde crosslinking system, with a particular focus on the influence of pH. In this system, formaldehyde acts directly as a reactant, and its quantity or concentration remains independent of the solution's pH. The experiments demonstrated that gelation occurs within a pH range of 1.0 to 8.5, with the crosslinking reaction proceeding rapidly at pH 1, while the rate of crosslinking is the slowest under neutral conditions. Feng et al. [39] utilized ^{13}C-NMR spectroscopy to explore the reaction process between PAM and formaldehyde. The study revealed that at high pH (9), formaldehyde reacts with PAM to produce N-hydroxymethylated polyacrylamide without leading to crosslinking. Conversely, at low pH (1), formaldehyde can react with PAM to form methylene-bis-acrylamide crosslinked structures. These findings indicate that pH plays a significant regulatory role in the crosslinking reaction between formaldehyde or phenolic formaldehyde crosslinking agents and acrylamide polymers.

 doi:10.20944/preprints202502.1604.v1

Marandi et al. [38] explored the crosslinking reaction of formaldehyde with PAM catalyzed by hydrochloric acid at pH 5. Under acidic condition, the protonation of the hydroxymethyl group facilitates the nucleophilic attack of amine nitrogen atoms on the carbon atoms of the hydroxymethyl groups, resulting in the formation of a gel structure with methylene diacrylamide serving as the crosslinking point. The crosslinking reaction proceeds via a nucleophilic reaction mechanism. In another study, melamine/formaldehyde (MF) resins rich in hydroxymethyl groups were used to crosslink HPAM [40], with optimal pH levels for stable, high-strength gels ranging from 5 to 9. Outside this range, gel viscosity decreases and strength weakens due to polymer chain coiling and hydrolysis. It is suggested that the reaction between the amide groups and the hydroxymethyl groups in the MF resin follows a nucleophilic substitution reaction mechanism. Acidic conditions promote the protonation of hydroxymethyl groups, thereby enhancing the crosslinking between amide groups and hydroxymethyl groups. Conversely, an increase in the pH of the reaction system inhibits the protonation of hydroxymethyl groups, which impedes the nucleophilic attack of the nitrogen atom in the amide group on the carbon of the hydroxymethyl group, ultimately preventing the establishment of a dense crosslinked network structure within the system.

Although a pH range of 5-9 is favorable for the formation of high-strength gels, acidic conditions can cause corrosion of the internal walls of the wellbore. To mitigate this issue, ammonium chloride was utilized as a catalyst to regulate the crosslinking reaction between HPAM and MF at pH levels of 8-9 [40]. At a temperature of 80 °C, this approach successfully reduced the gelation time from 7 days to a mere 8 hours, while simultaneously enhancing gel strength. It is suggested that the ammonium ions generated from the ionization of ammonium chloride donate protons to the hydroxymethyl groups, thereby accelerating the crosslinking reaction within the described system [40]. This study not only validates the nucleophilic substitution mechanism of the reaction between PAM and organic crosslinkers but also provides valuable insights for regulating gelation time based on this mechanism. References [45,46] have documented the use of ammonium salts to accelerate polymer gelation, particularly to facilitate the crosslinking reaction between polyacrylamide and phenolic formaldehyde compounds under low-temperature conditions. These findings will contribute to the rapid sealing of formations and the protection of oil and gas reservoirs during production activities.

Based on the nucleophilic substitution crosslinking reaction mechanism between PAM and phenolic formaldehyde compounds [38,40], this research employs urea additives to regulate both the gelation time and strength of the composite gel. Urea decomposes at elevated temperatures, producing ammonia and carbon dioxide, which further generate hydroxide and carbonate anions in the solution. These anions inhibit the protonation of the methylol group, thereby extending the gelation time of the gelant. Simultaneously, carbonate and hydroxide ions facilitate the precipitation of calcium and magnesium ions in brine, leading to the formation of inorganic particles and high-strength organic/inorganic composite gel. This study utilizes high-valent metal ions in formation brine as raw materials to in situ synthesize organic/inorganic composite gels. This approach not only mitigates the destabilizing impact of inorganic salts on polymer gels but also enhances the strength and stability of the composite gel through the incorporation of generated inorganic particles, thereby achieving integrated utilization of subsurface mineral resources.

2. Results and Discussion

In this study, urea was employed to regulate the crosslinking reaction between polyacrylamide and phenolic formaldehyde crosslinkers, as well as the precipitation reactions of calcium and magnesium ions. The amount of urea was carefully controlled to maintain a specific molar ratio between urea and the divalent metal ions in the solution, denoted as $N = n_{urea}/(n_{Ca^{2+}} + n_{Mg^{2+}})$, where n_{urea}, $n_{Ca^{2+}}$ and $n_{Mg^{2+}}$ are the amounts of substance of urea, calcium ions, and magnesium ions, respectively. The gelling solution or gelant transforms into an organic/inorganic composite gel (CG) with defined viscoelastic properties after high-temperature aging in the oven. For performance comparisons, freshwater gel (FG) and brine gel (BG) samples without urea were also prepared. In

 doi:10.20944/preprints202502.1604.v1

this paper, the samples of freshwater gel, brine gel, and composite gel are designated as FG-t, BG-T_x-t, and CG-T_x-U_N-t, respectively, where t signifies the aging temperature of the sample in degrees Celsius (°C), T_x indicates that the total dissolved solids or salinity in the gelant equals to $x\times10^4$ mg/L, and U_N represents the molar ratio *N* between urea and the sum of calcium and magnesium ions in the reaction system. Gel strength was recorded according to the Sydansk code method [8,47–49].

2.1. FT-IR and XRD

The FT-IR spectra of the PAM polymer and FG sample are presented in Figure 1a. The absorption peaks observed at 3443, 1641, and 1104 cm^{-1} correspond to the stretching vibrations of υ_{N-H}, $\upsilon_{C=O}$, and υ_{C-N}, respectively [9,18,40,50,51]. Furthermore, the peaks at 2920, 2851, 1453, and 1390 cm^{-1} represent the asymmetric stretching, symmetric stretching, asymmetric bending, and symmetric bending absorption peaks of the C-H bonds in the methylene group [9,18,50,51]. These findings confirm the presence of the primary functional groups in polyacrylamide. In the FT-IR spectrum of PAM FG sample, two new absorption peaks at 1570 and 1231 cm^{-1} appear, which are attributed to the stretching vibrations of carbon-carbon conjugated double bonds and the C-O bond stretching vibrations in phenolic compounds, respectively [50,52]. This FT-IR data suggests that a gel structure is formed through a crosslinking reaction between hydroquinone, formaldehyde, and PAM via covalent bonding.

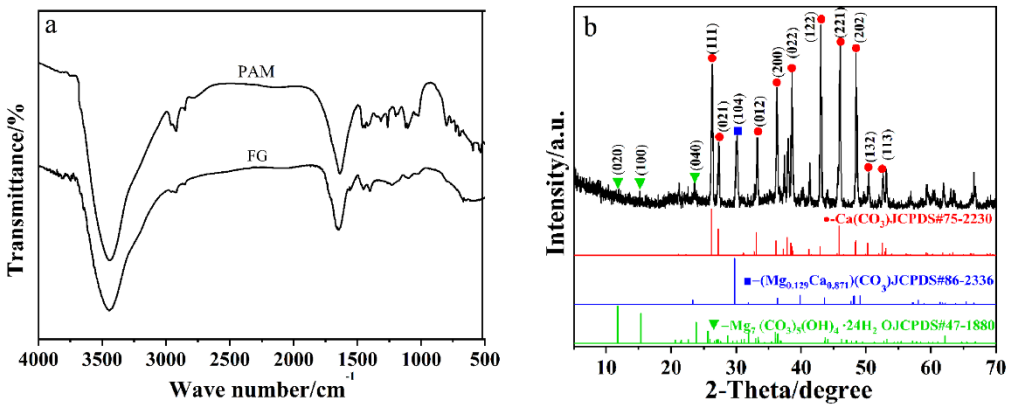

Figure 1. FR-IR spectra of PAM and FG (a), XRD curves of inorganic samples (b).

X-ray diffraction (XRD) is an effective technique for analyzing the structure of inorganic materials. In this study, XRD tests were conducted on inorganic particles formed by the reaction of Ca^{2+} and Mg^{2+} ions with hydrolysis products of urea, with the results illustrated in Figure 1b. The characteristic peaks observed at 2θ values of 26.1°, 27.4°, 33.4°, 36.1°, 38.7°, and 46.0° correspond to the (111), (021), (012), (200), (022), and (221) crystal plane diffractions of $CaCO_3$ (JCPDS#75-2230) [53]. A prominent peak at 2θ of 30.1° is attributed to the (104) crystal plane diffraction of $(Mg_{0.129}Ca_{0.871})CO_3$ (JCPDS#86-2336) [54]. The peaks at 2θ values of 12.0°, 15.2°, and 23.7° can be indexed as the (020), (100), and (040) crystal plane diffractions of $Mg_7(CO_3)_5(OH)_4{\cdot}24H_2O$ (JCPDS#47-188) [55]. The XRD results indicate that Ca^{2+} and Mg^{2+} ions in brine can react with OH^- and CO_3^{2-} generated from urea hydrolysis to form various inorganic particles, including calcium carbonate, magnesium calcium carbonate, and basic magnesium carbonate. The diffraction peak intensities of calcium carbonate and magnesium calcium carbonate are relatively strong, while the intensity of the basic magnesium carbonate peak is lower, suggesting that the crystal structures of the former two inorganic compounds are more well-defined, whereas basic magnesium carbonate exhibits significantly greater amorphicity [55]. The equations involving urea decomposition and its products further interacting with calcium and magnesium ions are detailed in Formulas (1) to (7) [56,57].

Urea decomposition reaction equations:

 doi:10.20944/preprints202502.1604.v1

$$CO(NH_2)_2+H_2O=CO_2\uparrow+2NH_3\uparrow \quad (1)$$

$$NH_3+H_2O\rightleftharpoons NH_3\cdot H_2O\rightleftharpoons NH_4^++OH^- \quad (2)$$

$$CO_2+H_2O=H_2CO_3\rightleftharpoons H^++HCO_3^- \quad (3)$$

$$HCO_3^- +OH^-\rightleftharpoons CO_3^{2-}+H_2O \quad (4)$$

Precipitation reaction equations for Ca^{2+} and Mg^{2+} ions:

$$CO_3^{2-} +Ca^{2+}\rightarrow CaCO_3 \quad (5)$$

$$CO_3^{2-} +0.129Mg^{2+}+0.871Ca^{2+}\rightarrow (Mg_{0.129}\ Ca_{0.871})CO_3 \quad (6)$$

$$5CO_3^{2-} +7Mg^{2+}+4OH^-+24H_2O\rightarrow Mg_7(CO_3)_5(OH)_4\cdot 24\ H_2O \quad (7)$$

The amide groups in PAM undergo hydrolysis at elevated temperatures, leading to the formation of carboxyl groups, which subsequently dissociate into carboxylate ions that interact with cations in the solution through electrostatic or coordination forces [1,8,36,58]. The electrostatic interactions between Ca^{2+} and Mg^{2+} ions and carboxylate ions in the solution are significantly stronger than those with monovalent cations. Additionally, divalent cations can bind to carboxylate ions from different molecular chains, resulting in crosslinking that reduces the hydrophilicity of the polymer, and may even lead to excessive crosslinking and syneresis [1,36,58]. This phenomenon is a major contributor to the reduced stability of the polymer under high mineralization conditions. In PAM solutions with a high concentration of Ca^{2+} and Mg^{2+} ions, the availability of carboxylate ions is relatively limited, meaning that only a fraction of the divalent ions can interact with carboxylate ions through electrostatic or coordination interactions. At elevated temperatures, urea decomposes to produce NH_3 and CO_2. As the concentration of NH_3 increases within the reaction system, it further reacts with water to yield NH_4^+ and OH^-, resulting in an increase in the system's alkalinity. Concurrently, CO_2 can generate carbonate ions (CO_3^{2-}) under alkaline conditions. The cations Ca^{2+} and Mg^{2+} that associate with carboxylate ions can precipitate with OH^- and CO_3^{2-} on the surface of the polymer, leading to the formation of inorganic particles such as calcium carbonate, magnesium carbonate, and basic magnesium carbonate. This process resembles biomineralization [59]. These inorganic particles interact with the carboxylate ions of the polymer through electrostatic or coordination forces, resulting in the formation of an organic/inorganic composite gel. Scheme 1 illustrates the deposition of calcium and magnesium inorganic particles on the surface of polyacrylamide.

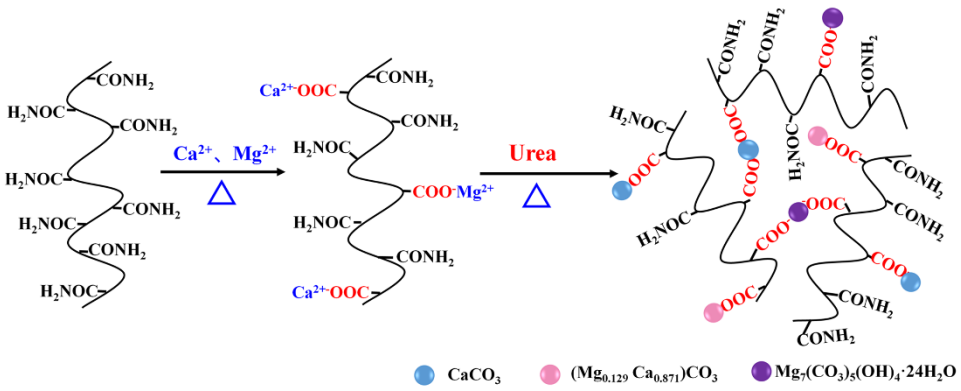

Scheme 1. Schematic diagram of inorganic particles deposited on the surface of polyacrylamide.

2.2. SEM

The experimental results reveal that both the BG sample (BG-T_{15}-95, Figure 2a) and CG sample (CG-T_{15}-$U_{1.00}$-95, Figure 2d) exhibit a three-dimensional network morphology. During the freeze-

 doi:10.20944/preprints202502.1604.v1

drying process, a substantial amount of inorganic salts precipitates continuously on the surface of the crosslinked polymer network in both gels. Figure 2b and Figure 2e display the SEM images of the BG and CG samples after being washed with water, respectively. While the gel samples maintain their three-dimensional network structure, the surface of the polymer gel becomes smoother after washing, indicating the removal of water-soluble inorganic salts. Upon further magnification of the electron microscope images, it was observed that no significant particles were attached to the surface of the polymer in the BG sample (Figure 2c). In contrast, numerous solid particles remained adhered to the surface of the polymer in the CG sample (Figure 2f), with an average particle size of approximately 80-100 nm. This morphological characteristic is similar to that of the PAM/PEI/CAF composite gels [26]. It is inferred that the solid particles attached to the polymer surface in the composite gel correspond to inorganic particles of calcium carbonate, magnesium carbonate, or basic magnesium carbonate, as indicated by the XRD test results. These insoluble substances, formed from calcium and magnesium ions in conjunction with the decomposition products of urea, cannot be removed through water washing. Moreover, electrostatic or coordination interactions between divalent cations and the carboxylate anions of the polymer facilitate the stable adhesion of the particles to the polymer surface. Consequently, the crosslinked polymer forms an organic/inorganic composite gel with the inorganic particles.

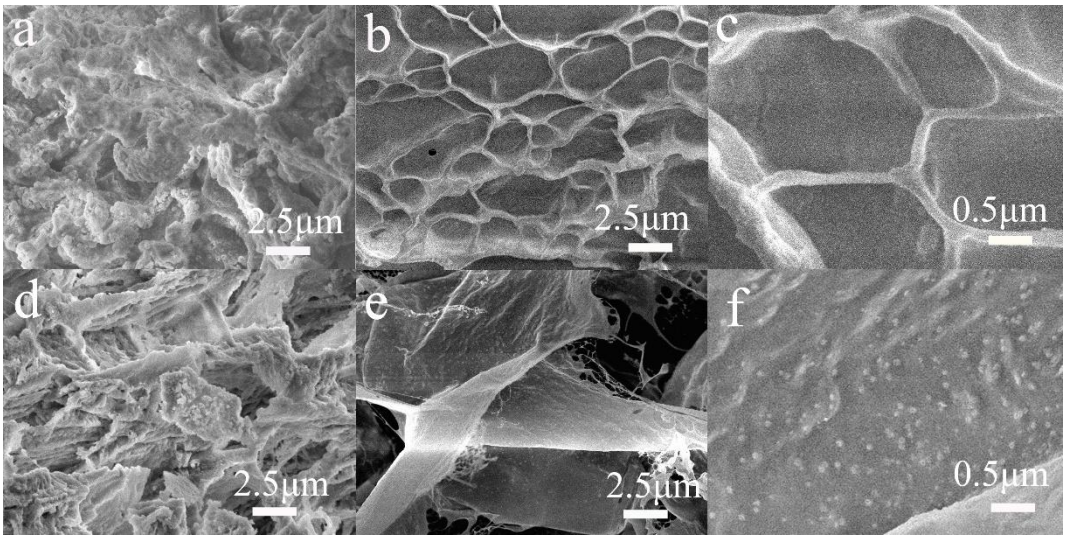

Figure 2. SEM images of BG-T_{15}-95(a-c) and CG-T_{15}-$U_{1.00}$-95(d-e). a, d (without washing); b, e (after washing); c, e (magnified images after washing).

PAM is a linear polymer that undergoes a crosslinking reaction involving its amide groups when exposed to phenolic formaldehyde crosslinking agents, resulting in the development of a three-dimensional gel network. When a substantial amount of sodium chloride, calcium chloride, and magnesium chloride is dissolved in water, a three-dimensional brine gel is formed. According to the salinity composition of the brine gel, a certain amount of urea is introduced into the reaction system. Under high-temperature conditions, urea decomposes and facilitates the precipitation reaction of divalent cations, leading to the formation of inorganic particles such as calcium carbonate, magnesium carbonate, and basic magnesium carbonate. These inorganic components interact with the organically crosslinked polymer, resulting in the creation of a three-dimensional composite gel. The precipitation reaction consumes a significant amount of high-valent metal ions, thereby reducing their concentrations in the liquid phase and effectively mitigating their adverse effects on the stability of the polymer gel. Concurrently, the inorganic particles are uniformly distributed within the crosslinked polymer matrix, significantly enhancing the elastic modulus, strength, and stability of the composite gel [16,17,26,28].

2.3. Gelation Performance

 doi:10.20944/preprints202502.1604.v1

The gelation process and stability of gel samples were recorded based on the gel strength codes proposed by Sydansk et al. [8,47–49]. The classification of gel strength levels is detailed in Table 1. The gel strength developments of FG, BG, and CG samples throughout the gelation process at temperatures of 95 °C and 120 °C, are presented in Tables 2 and Table 3. The FG can achieve a maximum strength of I at 95 °C without syneresis. At 120 °C, FG can also reach the strength of I level, but begins to dehydrate after being heated for 126 days. BG samples similarly attain their maximum strength I at 95 °C. However, brine gels exhibit a highest strength of H and these samples are more susceptible to dehydration at 120 °C. CG samples demonstrate the capability to reach a peak strength of I at both 95 °C and 120 °C. Moreover, the CG samples show superior stability under higher urea proportion conditions (N=1.0-2.0).

Table 1. Gel strength code and description.

gel strength code	description
A	No detectable gel formed: The viscosity of the gelant is as same as that of polymer solution.
B	Highly flowable gel: The viscosity of the gelant is slightly higher than that of the initial polymer solution.
C	Flowable gel: The majority of the gelant can flow upon inversion.
D	Medium flowable gel: 90-95% of the gel can flow upon inversion.
E	Slightly flowable gel: less than 85% of the gel can flow upon inversion.
F	Highly deformable gel: The gel is highly deformed but does not flow upon inversion.
G	Moderately deformable gel: The gel does not flow and the gel deforms to the middle of the bottle upon inversion.
H	Slightly deformable gel: The gel does not flow and only the surface of the gel undergoes slight deformation upon inversion.
I	Rigid gel: The surface of the gel does not deform upon inversion.

Table 2. Gel sample strength code at different time (95 °C).

samples	time/d																			
	0.	2.	4.	5.	6.	7.	8.	9.	9.	11	12	14	24	35	36	40	42	78	1	1
FG-95	A	B	B	B	B	B	B	D	D	F	G	H	I	I	I	I	I	I	I	I
BG-	A	A	B	B	B	B	B	B	B	C	D	E	F	H	I	I^{3}	I^{5}	/	/	/
BG-	A	A	B	B	B	B	B	B	B	D	D	E	I	$I^{0.5}$	I^{1}	I^{5}	/	/	/	/
BG-	A	B	B	B	B	C	D	E	E	F	F	F	H	H^{5}	/	/	/	/	/	/
BG-	A	B	B	B	C	D	E	F	F	H	H	$H^{0.5}$	H^{5}	/	/	/	/	/	/	/
CG-	A	D	H	I	I	I	I	I	I	I	I	$I^{0.1}$	$F^{0.5}$	F^{4}	F^{5}	/	/	/	/	/
CG-	A	B	D	E	H	H	H	I	I	I	I	I	I	I	I	I	I	I^{5}	/	/
CG-	A	B	C	D	G	G	H	I	I	I	I	I	I	I	I	I	I	I	I^{5}	/
CG-	A	B	B	C	D	F	G	I	I	I	I	I	I	I	I	I	I	I	I	I
CG-	A	B	B	B	B	B	B	C	D	E	F	F	I	I	I	I	I	I	I	I
CG-	A	B	B	B	B	B	B	B	B	B	C	D	I	I	I	I	I	I	I	I

* The superscript number on the right of the gel strength symbol represents the dehydration volume of the gel sample, in mL. Stop observation when the dehydration reaches 5 mL.

Table 3. Gel sample strength code at different time (120 °C).

samples	time/d																		
	0.	1.	1.	1.	2.	2.	2.	3.	4.	5.	6.	7.	9.	14.	15.	20.	31.	12	13
FG-	A	B	B	B	C	D	D	D	H	H	H	I	I	I	I	I	I	$I^{0.2}$	$I^{0.2}$

 doi:10.20944/preprints202502.1604.v1

BG-T5-	A	B	B	B	B	C	C	D	G	H^{0}	H^{0}	H^{0}	H	H^{4}	H^{5}	/	/	/	/
BG-	A	B	B	B	B	C	D	G	G	H^{0}	H^{0}	H^{1}	H	H^{5}	/	/	/	/	/
BG-	A	B	B	B	D	F	F	F	F^{0}	$F^{0.}$	F^{1}	F^{3}	F^{5}	/	/	/	/	/	/
BG-	A	B	C	D	F	G	G	G	H	H^{0}	H^{1}	H^{5}	/	/	/	/	/	/	/
CG-	A	D	H	H	F^{0}	F^{0}	F^{0}	F^{0}	F^{0}	F^{1}	F^{2}	$F^{2.}$	F^{5}	/	/	/	/	/	/
CG-	A	B	D	D	F	G	G	H	I	I	I	I	$I^{0.}$	$I^{0.5}$	I^{1}	I^{5}	/	/	/
CG-	A	B	C	D	E	F	F	F	G	G	G	H	$I^{0.}$	$I^{0.5}$	H^{1}	H^{2}	H^{5}	/	/
CG-	A	B	B	B	B	C	D	D	F	G	H	H	H	H	I	I	I	I^{2}	$I^{2.5}$
CG-	A	B	B	B	B	B	B	B	C	D	G	H	H	H	I	I	I	I^{1}	$I^{1.5}$
CG-	A	B	B	B	B	B	B	B	B	C	D	F	G	H	I	I	I	$I^{0.5}$	$I^{0.8}$

* The superscript number on the right of the gel strength symbol represents the dehydration volume of the gel sample, in mL. Stop observation when the dehydration reaches 5 mL.

The time required for the gel sample to attain a strength code of D was recorded as the gelation time (t_D) [48,49]. The stability time (t_S) is defined as the duration needed for the gel to dehydrate by 5 mL from 20 mL gel sample. This work conducts a comparative analysis of the effects of various factors, including urea concentration (C_{urea}), degree of mineralization, and temperature, on both t_D and t_S.

t_D and t_S data of FG and BG samples are shown in Table 4. Experimental results indicate that at 95 °C and 120 °C, the gelation times of FG are 9.7 days and 2.7 days, respectively, demonstrating that gelation time decreases with increasing temperature. The stability times of FG at both temperatures exceed 176 days and 126 days, respectively. At these temperatures, when the salinity of the gelant is set between 5 and 20×10⁴ mg/L, both gelation time and stability period of the BG samples gradually decline as salinity increases. At 95 °C, the gelation time of BG samples decreases from 12.4 days to 7.9 days, while stability time drops from 42.0 days to 24.5 days. At 120 °C, the gelation time of BG samples reduces from 3.0 days to 1.9 days, and stability time decreases from 15.8 days to 7.5 days. Notably, BG samples exhibit significantly shorter stability times compared to FG samples. When comparing high-temperature samples with low-temperature samples, both gelation time and stability time are shorter for the former. These findings suggest that high temperature and high salinity are the primary factors contributing to the reduced stability of polymer gels [1,8,36,37,58]. Under high-temperature conditions, the thermal motion of polymer and crosslinking agent molecules intensifies, providing higher energy that enables more molecules to participate in the crosslinking reaction, thereby shortening the gelation time [10,16,26]. Under high mineralization conditions, divalent calcium and magnesium ions facilitate polymer hydrolysis, converting amide groups into carboxyl groups, which can further dissociate into carboxylate ions and hydrogen ions. Divalent cations link with carboxylate ions of different polymer chains through ionic interactions [58], while the dissociated hydrogen ions promote nucleophilic substitution crosslinking reactions between amide groups and phenolic formaldehyde crosslinking agents. These result in over-crosslinking and syneresis within the system, significantly diminishing the stability of the gel samples [36,37,58,60].

Table 4. Gelation time (t_D) and stability time (t_S) of FG, BG samples.

samples	t_D/d	t_S/d
FG-95	9.7	>176
BG-T5-95	12.4	42.0
BG-T10-95	11.2	40.8
BG-T15-95	8.4	35.0
BG-T20-95	7.9	24.5
FG-120	2.7	>126
BG-T5-120	3.0	15.8

 doi:10.20944/preprints202502.1604.v1

BG-T_{10}-120	2.9	14.3
BG-T_{15}-120	2.3	9.7
BG-T_{20}-120	1.9	7.5

*At 95 °C, C_{PAM} = 1.0 wt%, C_{HQ} = 0.20 wt%, C_{HCHO} = 0.21 wt%； At 120 °C, C_{PAM} = 1.0 wt%, C_{HQ} = C_{HCHO} = 0.16wt %.

At 95 °C, we examined the impact of polymer concentration and crosslinking agent concentration on the gelation time and stability of the composite gel with a salinity of 15×10⁴ mg/L and a fixed urea concentration of 0.68 wt% (*N*=0.5). The experimental data are summarized in Table 5. The results reveal that when the concentrations of C_{PAM}, C_{HQ} and C_{HCHO} are maintained at 0.5-2.0 wt%, 0.06-0.31 wt%, and 0.07-0.33 wt%, respectively, the gel structure formed at low polymer concentration (0.5 wt%) and low crosslinking agent concentration (0.06 wt%, 0.07 wt%) is incomplete and susceptible to dehydration. In contrast, when the PAM concentration is excessively high (1.5-2.0 wt%), the gelation time is significantly reduced to 0.7-1.2 days, resulting in over-crosslinking, syneresis, and a loss of stability. Consequently, the optimized concentrations for C_{PAM}, C_{HQ} and C_{HCHO} at 95 °C are determined to be 1 wt%, 0.20 wt%, and 0.21 wt%, respectively. At 120 °C, the preferred C_{PAM} remains at 1 wt%, while both C_{HQ} and C_{HCHO} are adjusted to 0.16 wt% to delay the crosslinking reaction.

Table 5. Effects of polymer concentration and crosslinker concentration on gelation time and stability time of composite gel CG-T_{15}-$U_{0.5}$-95.

C_{PAM}/%	C_{HQ}/wt%	C_{HCHO}/wt%	t_D/d	t_S/d
1.0	0.06	0.07	12.6	69.2
1.0	0.12	0.14	7.7	71.0
1.0	0.20	0.21	4.6	78.0
1.0	0.25	0.27	1.9	56.1
1.0	0.31	0.33	1.6	43.9
0.5	0.20	0.21	9.1	37.8
1.5	0.20	0.21	1.2	57.0
2.0	0.20	0.21	0.7	57.0

To further investigate the effects of salinity and C_{urea} on the gelation performance of the composite gel, we examined urea-containing crosslinking systems with *N* values of 0.5 and 1.0 across salinities ranging from 5 to 20×10⁴ mg/L. The gelation time and stability performance of the composite gels are presented in Table 6. Due to the proportional amount of urea and divalent cations in the reaction solution, C_{urea} increases along with salinity, leading to a gradual extension of the gelation time for the composite gel. When *N* is set at 0.5, an increase in salinity results in an extended gelation time from 2.1 days to 5.2 days, with stability times ranging from 72.1 to 85.2 days, significantly surpassing those of the brine gel. When the *N* value is increased to 1.0, as salinity rises from 5 to 20×10⁴ mg/L, the gelation time extends from 2.2 days to 7.0 days, while the stability time of the composite gel further increases to over 155.0 days. These findings underscore the critical role of urea in delaying the crosslinking reaction between polyacrylamide and the phenolic formaldehyde crosslinker at elevated temperatures, thereby enhancing the stability of the composite gel.

Table 6. Effects of salinity and urea concentration on gelation time and stability time of composite gels.

samples	C_{urea}/wt%	t_D/d	t_S/d
CG-T_5- $U_{0.50}$-95	0.23	2.1	85.2
CG-T_{10}- $U_{0.5}$-95	0.45	2.8	76.7

 doi:10.20944/preprints202502.1604.v1

CG-T_{15}- $U_{0.5}$-95	0.68	4.6	78.0
CG-T_{20}- $U_{0.5}$-95	0.90	5.2	72.1
CG-T_{5}- $U_{1.0}$-95	0.45	2.2	167.4
CG-T_{10}- $U_{1.0}$-95	0.90	3.6	161.2
CG-T_{15}- $U_{1.0}$-95	1.35	6.6	155.0
CG-T_{20}- $U_{1.0}$-95	1.81	7.0	170.0

This paper systematically investigates the effects of C_{urea} on the gelation and stability times of a polymer solution with a salinity of 15×10^4 mg/L and a PAM concentration of 1 wt% at temperatures of 95 °C and 120 °C, as illustrated in Figure 3. The findings reveal that by adjusting the N value between 0.1 and 2.0, the mass percentage of urea in the gel reaction fluid varies from 0.14 to 2.71 wt%, as indicated on the horizontal axis of Figure 3. An increase in urea concentration results in gelation times ranging from 2.5 to 14.1 days at 95 °C and from 1.4 to 6.5 days at 120 °C (Figure 3a), demonstrating that urea effectively regulates the gelation time t_D of the composite gel. Although the t_D at 120 °C is shorter than that at 95 °C, higher urea concentrations can extend the t_D by 3.6 to 4.6 times, leading to significantly longer gelation times for CG samples compared to FG and BG specimens.

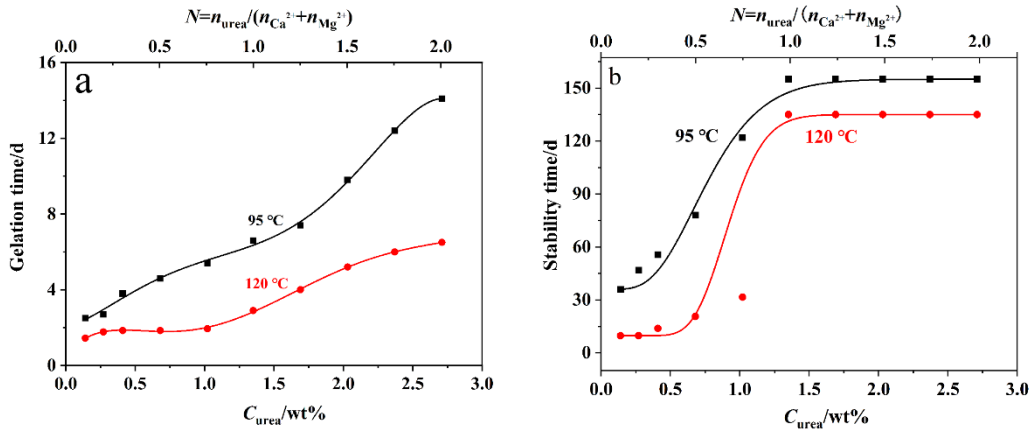

Figure 3. CG gelation time (a) and stability time (b) curves vs. C_{urea} at 95 °C and 120 °C. Total dissolved solids and C_{PAM} are 15×10^4 mg/L and 1%, respectively.

In both laboratory experiments and field production, a common approach to prolong gelation time is to adjust the concentrations of crosslinking agents and polymers. For instance, references [12–14] indicate that adjustable gelation time ranges are 21-41 hours at 100.8 °C, 6.3-15.5 hours at 110 °C, and 7-14 hours at 150 °C. Although these regulatory measures demonstrate some effectiveness, the overall findings highlight that short gelation times and limited controllable ranges at elevated temperatures remain significant technical challenges. A comprehensive understanding of the crosslinking reaction mechanism, coupled with precise regulation of the concentrations of reaction components, is crucial for effectively extending the high-temperature crosslinking reaction time of the polymer.

In this paper, urea is employed as a base source. At high temperatures, it decomposes into ammonia and carbon dioxide. This process leads to the formation of weak electrolytes, such as hydrated ammonia and carbonic acid, which partially dissociate into NH_4^+, OH^-, H^+, HCO_3^- and CO_3^{2-} ions. The anions interact with NH_4^+ and H^+ ions through electrostatic forces, effectively suppressing the protonation of hydroxymethyl groups and thereby prolonging the crosslinking reaction time at elevated temperatures [40]. The ionization equilibrium of the weak electrolyte shifts forward only when Ca^{2+} and Mg^{2+} ions in the solution consume a sufficient amount of OH^- and CO_3^{2-} ions, allowing NH_4^+ and H^+ ions to facilitate the crosslinking reaction. Based on the nucleophilic reaction

 doi:10.20944/preprints202502.1604.v1

mechanism, the gelation time of the PAM solution can be extended, thereby creating favorable conditions for deep profile control and water plugging in oilfields.

Figure 3b illustrates the correlation between the stability time t_S of the composite gel and the urea concentration C_{urea}. At 95 °C, it is clear that as C_{urea} increases from 0.14 wt% (N=0.1) to 0.41 wt% (N=0.3), the stability time of the composite gel extends from 36.0 days to 55.7 days. Further increasing C_{urea} to 0.68 wt% (N =0.5) and 1.02 wt% (N=0.75) results in a significant increase in stability time, reaching 78 days and 122 days, respectively. Notably, when C_{urea} is elevated to the range of 1.35-2.71 wt% (N=1.0-2.0), the stability time can extend up to 155 days. At 120 °C, the stability time of the composite gel is slightly reduced compared to that at 95 °C. Specifically, as C_{urea} increases from 0.14 wt% (N=0.1) to 1.02 wt% (N=0.75), the stability time gradually rises from 9.75 days to 31.6 days. This trend suggests that high-temperature conditions may lead to over-crosslinking and syneresis, which can reduce stability time. However, further increasing C_{urea} significantly prolongs the stability time of the composite gel at 120 °C. For example, when C_{urea} increases from 1.35 wt% (N=1.0) to 2.71 wt% (N=2.0), the stability time of the composite gel samples can reach 135 days.

Urea facilitates the precipitation of Ca^{2+} and Mg^{2+} ions, leading to the formation of carbonate particles. This process not only effectively reduces the concentration of divalent cations that undermine gel stability but also enhances the stability of the composite gel by incorporating inorganic particles. Under the influence of urea, the stability time of the composite gel significantly increases, allowing it to maintain strength at I or H levels for an extended period under high-temperature and high-salinity conditions (Table 2 and Table 3). This stability is crucial for improving production efficiency in oilfields.

2.4. Dynamic Rheological Property

It is well established that during the aging process of the gelant, urea gradually decomposes, and the alkaline environment effectively inhibits hydroxymethyl protonation, thereby extending the gelation time at elevated temperatures. Concurrently, the OH^- and CO_3^{2-} anions present in the reaction system can precipitate with Ca^{2+} and Mg^{2+} ions in highly mineralized solutions, leading to the formation of inorganic particles that subsequently create organic/inorganic composite gels with the crosslinked polymers. To analyze the impact of the composite structure on gel strength, this study evaluated the dynamic rheological properties of the gel samples. The elastic modulus and viscous modulus of FG, BG, and CG samples were measured, and the effects of urea concentration and salinity on gel performance were assessed, as illustrated in Figure 4.

 doi:10.20944/preprints202502.1604.v1

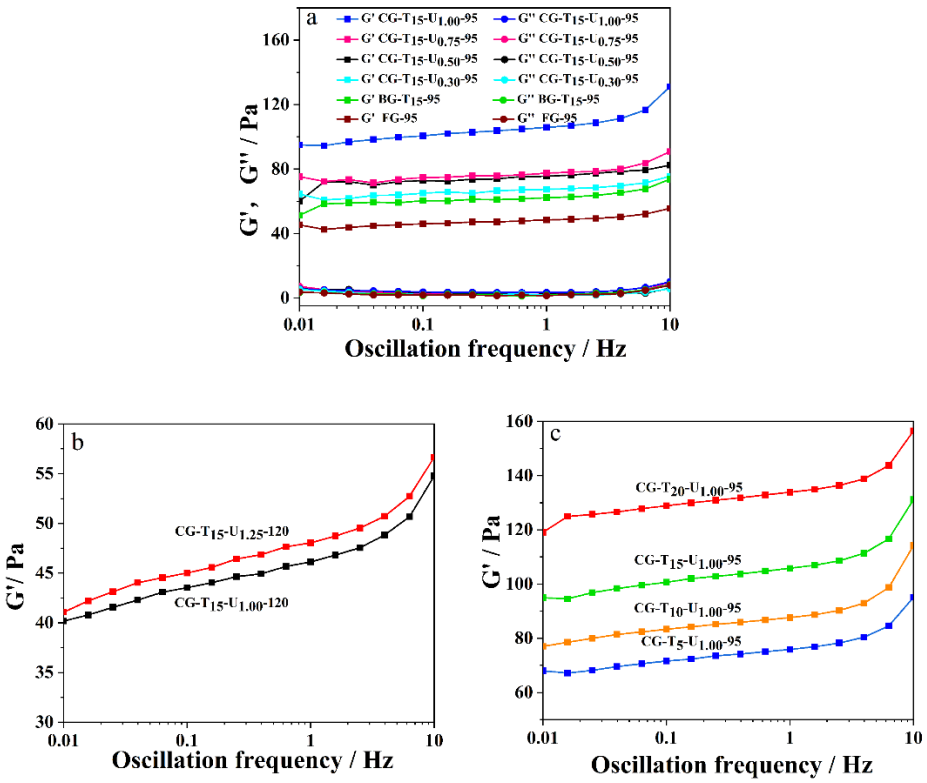

Figure 4. Elastic modulus and viscous modulus of gel samples at 95 °C (a), elastic modulus of gel samples at 120 °C (b), effects of salinity on the elastic modulus of CG samples at 95 °C (c).

Figure 4a illustrates the elastic modulus and the viscous modulus curves of FG, BG, and CG samples. The composite gels were prepared under varying urea concentration conditions, with a salinity of 15×10^4 mg/L. All samples were aged at 95 °C for 44.7 days. Firstly, the overall experimental results indicate that the elastic modulus G′ of all gel samples is significantly greater than the viscous modulus G″, demonstrating that the gel networks formed through crosslinking reactions possess excellent deformation characteristics and quasi-solid properties [21,31,61], which aid in plugging large pores in the formation and controlling the water absorption profile. Secondly, under experimental conditions with oscillation frequencies ranging from 0.01 to 10 Hz, the elastic modulus G′ of the freshwater gel FG-95 is the lowest (45.3-55.6 Pa), followed by the brine gel BG-T15-95 (51.3-73.7 Pa), while the composite gel exhibits the highest elastic modulus (Figure 4a). It can be analyzed that, although the polymer molecular chains in the FG system are the most extended, the strength of the pure organic gel is the lowest. In contrast, the BG containing inorganic salts demonstrates a higher elastic modulus than the FG under the same conditions, attributed to calcium and magnesium ions promoting the hydrolysis of PAM and crosslinking with the formed carboxylate groups [1,8,36], thereby enhancing the gel strength. When urea is introduced into the reaction solution, the inorganic particles in the prepared composite gel interact with the polymers through electrostatic or coordination forces, and this composite structure imparts a higher elastic modulus to the product [16,17]. It is evident that both the crosslinked structure and the composite structure directly influence the enhancement of gel strength. Thirdly, the elastic modulus of the composite gel increases with rising urea concentration. In Figure 4a, there are four CG samples including CG-T_{15}-$U_{0.30}$-95, CG-T_{15}-$U_{0.50}$-95, CG-T_{15}-$U_{0.75}$-95, and CG-T_{15}-$U_{1.00}$-95. The salinity and polymer concentration were fixed at 15×10^4 mg/L and 1 wt%, respectively. As the *N* value increases from 0.30 to 1.00, the elastic modulus ranges for the four CG samples are 64.5-75.6 Pa, 60.0-82.4 Pa, 75.2-90.9 Pa, and 94.9-131.2 Pa, respectively. These results indicate that the elastic modulus of CG-T_{15}-$U_{0.30}$-95 is slightly higher than that of BG-T_{15}-95 (51.3-73.7 Pa). As the *N* value further increases to 0.50 and 0.75, the strengths of these two composite gel samples rise, showing an increase of 10-15 Pa in elastic modulus compared to that of CG-T_{15}-$U_{0.30}$-95. When the *N* value reaches 1.00 in sample CG-T_{15}-$U_{1.00}$-95, there is a

 doi:10.20944/preprints202502.1604.v1

significant increase in gel strength, approximately 20-40 Pa. This is attributed to the relatively high number of inorganic particles formed by calcium and magnesium ions under this condition, further enhancing the structure and strength of the composite gel [17,21,26].

Figure 4b shows the variation of the elastic modulus of the composite gels of CG-T_{15}-$U_{1.00}$-120 and CG-T_{15}-$U_{1.25}$-120. They were prepared at 120 °C with an aging time of 7.3 days. The experimental results indicate that as C_{urea} increases from 1.35 wt% to 1.69 wt% (N value increasing from 1.0 to 1.25), the elastic modulus of the CG ranges from 40.2 to 54.8 Pa and from 41.1 to 56.6 Pa, respectively. This slight increase in elastic modulus suggests that C_{urea} in the reaction system is already adequate. In Figure 4b, the elastic modulus of the CG sample CG-T_{15}-$U_{1.00}$-120 (120 °C, aged for 7.3 days, C_{PAM} = 1.0 wt%, C_{HQ} = 0.20 wt%, C_{HCHO} = 0.21 wt%) is lower than that of the CG sample CG-T_{15}-$U_{1.00}$-95 depicted in Figure 4a (95 °C, aged for 44.7 days, C_{PAM} = 1.0 wt%, C_{HQ} = C_{HCHO} = 0.16 wt%). This discrepancy is attributed to the different aging times and concentrations of crosslinking agents in the two gel systems. At 120 °C, the concentration of crosslinking agents is lower, and the aging time is also shorter, leading to reduced gel strength. In fact, delaying the gelation rate of the gel system under high-temperature conditions and controlling the increase in gel strength is more advantageous for the gelant to penetrate deeply into the formation. Furthermore, as indicated in Table 3, the CG samples under high-temperature conditions demonstrate long-term stability, with gel strength reaching level I.

Figure 4c depicts the elastic modulus of composite gel samples, ie, CG-T_5-$U_{1.00}$-95, CG-T_{10}-$U_{1.00}$-95, CG-T_{15}-$U_{1.00}$-95, and CG-T_{20}-$U_{1.00}$-95. As salinity and urea concentration increase, the elastic modulus of the composite gel increases correspondingly. For salinities of 5, 10, 15, and 20 ×10^4 mg/L, the elastic modulus ranges for the CG samples are 68.0-95.1 Pa, 77.0-114.2 Pa, 94.9-131.2 Pa, and 119.1-156.4 Pa, respectively. These results confirm the role of inorganic particles formed in brine in enhancing the elastic modulus of the composite gel. Increased urea concentrations and salinities result in a higher quantity of inorganic particles in the system, thus strengthening the composite gel [17,21,26]. This study employs a precipitation reaction between products of urea decomposition and calcium and magnesium ions to treat inorganic salts, converting destabilizing metal ions into beneficial inorganic particles. Simultaneously, these generated inorganic particles are used to construct the composite gel in situ with organic crosslinked polymers, thereby improving its elastic modulus. This process exemplifies an effective integration of inorganic salt treatment and application, converting adverse factors that destabilize the gel into favorable conditions that improve its strength and stability. This research has introduced a novel and efficient method for the in situ preparation of organic/inorganic composite gels from concentrated brine.

2.5. Thermal Stability

Figure 5 presents the thermogravimetric (TG), differential scanning calorimetry (DSC), and differential thermogravimetric (DTG) curves for FG, BG, and CG samples. The thermal analysis is divided into low-, medium-, and high-temperature ranges based on the weight loss observed in the DTG curves, as illustrated in Figure 5. The primary changes within each temperature range are summarized as follows. In the low-temperature range, adsorbed water is desorbed from the gel samples [16,17,62]. Within the medium-temperature range, imidization reactions occur through pendant amide groups [16,62–64], marking the onset of significant structural changes in the polymer. In the high-temperature range, processes such as polymer backbone cleavage, gel crosslinking bond breakage, and inorganic decomposition are evident [9,62–64]. The thermal decomposition temperature serves as a critical threshold at which the gel samples start to lose thermal stability.

 doi:10.20944/preprints202502.1604.v1

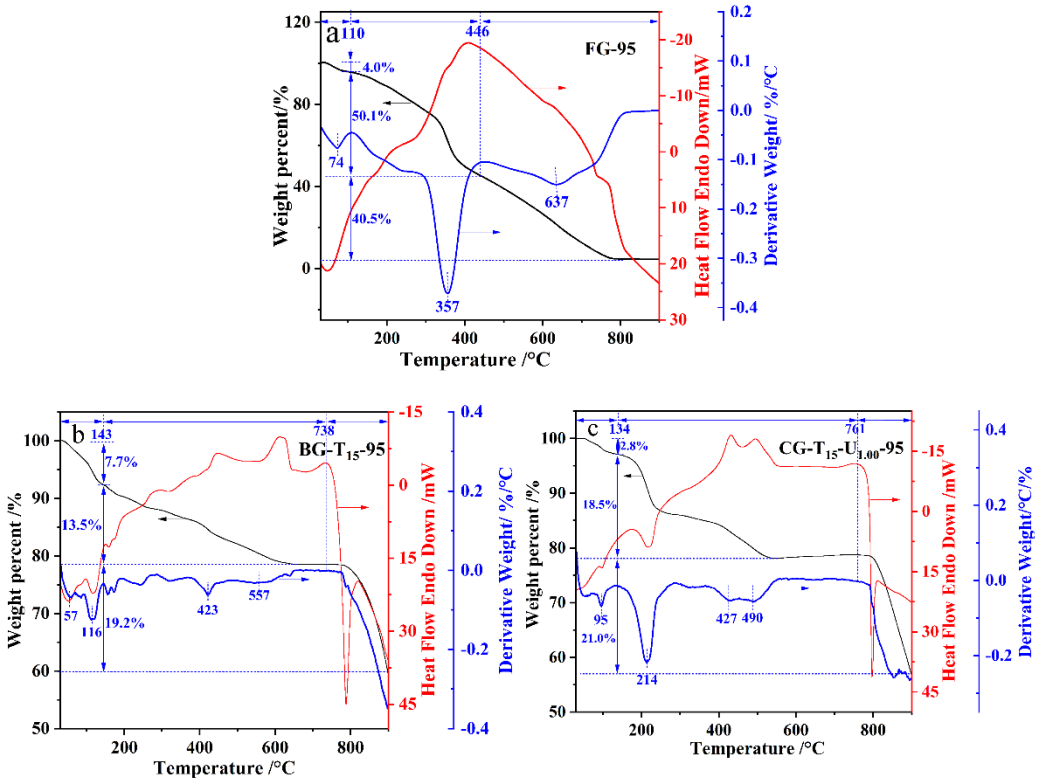

Figure 5. TG-DSC-DTG curves of FG (a), BG (b) and CG (c).

For the freshwater gel sample FG-95 (Figure 5a), dehydration occurs over a temperature range of 30-110 °C, with the peak weight loss rate at approximately 74 °C, resulting in a weight reduction of about 4.0%. For the BG-T15-95 sample (Figure 5b), dehydration spans from 30 to 143 °C, featuring notable weight losses at around 57, 85, and 116 °C. The weight loss at 116 °C corresponds to the removal of adsorbed water from magnesium salts in the brine gel [65], indicating a higher dehydration temperature relative to FG, with a total weight loss of 7.7%. In the case of the CG-T15-U1.00-95 sample (Figure 5c), dehydration occurs between 30 and 134 °C, with the maximum weight loss rate peaking around 95 °C, leading to a weight loss of approximately 2.8%. This lower weight loss suggests a reduced hydrophilicity of the inorganic components in the composite gel. The DSC curves for all gel samples during the dehydration process exhibit endothermic behavior, reflecting the energy absorbed during these transformations.

The imidization reactions for FG, BG, and CG samples occur within moderate temperature ranges of 110-446 °C, 143-738 °C, and 134-761 °C, respectively. The DSC curves for these processes exhibit exothermic behavior. Side-chain decomposition in FG, BG, and CG predominantly takes place at 357 °C, 423 °C and 427 °C. The notably higher thermal decomposition temperatures of BG and CG compared to FG suggest an improvement in thermal stability attributed to the incorporation of inorganic materials. An additional weight loss around 214 °C is noted for the composite gel sample (Figure 5c), which is indicative of the endothermic dehydration of basic magnesium carbonate [66].

In the high-temperature range from 446-900 °C for FG, 738-900 °C for BG, and 761-900 °C for CG, the DSC curves show endothermic events corresponding to the decomposition of the polymer main chain, rupture of crosslinking bonds within the gel, and decomposition of inorganic components. While FG exhibits substantial decomposition around 637 °C, nearly reaching completion by 900 °C (Figure 5a), BG and CG undergo significant decomposition only beyond their respective onset temperatures of 738 °C and 761 °C (Figure 5b, 5c). Consequently, due to the presence of inorganic constituents, BG and CG retain residual masses of 59.6% and 57.7%, respectively, at 900 °C.

 doi:10.20944/preprints202502.1604.v1

3. Conclusions

This study innovatively employs urea as a precipitating agent to synthesize organic/inorganic composite gels, with low molecular weight PAM as the primary agent, HQ and formaldehyde serving as crosslinking agents. The decomposition of urea not only inhibits nucleophilic substitution reactions, thereby extending the gelation time, but also promotes the in situ transformation of destabilizing calcium and magnesium ions into stable inorganic particles such as calcium carbonate, magnesium carbonate, and basic magnesium carbonate. Consequently, the interplay between the organic and inorganic components results in a robust three-dimensional composite structure that significantly enhances the mechanical strength and stability of the gel.

The gelation time for these composite materials can be precisely controlled within a range of 6.6 to 14.1 days at 95 °C and 2.9 to 6.5 days at 120 °C, with stability durations reaching 155 days and 135 days, respectively. This work pioneers an efficient method for the in situ preparation of organic/inorganic composite gels, exploiting urea's unique ability to delay high-temperature crosslinking reactions of PAM while simultaneously addressing the challenge posed by high salinity inorganic salts present in formation waters. The resulting heat-resistant and salt-tolerant composite gels represent a significant advancement in material science, offering valuable insights for profile control and water shut-off operations in high-temperature, high-salinity reservoirs.

4. Materials and Methods

4.1. Materials

The reagents employed in the experimental process, including acrylamide (AM), potassium persulfate ($K_2S_2O_8$), urea, hydroquinone (HQ), formaldehyde (37 wt%), sodium chloride, magnesium chloride, and hexahydrate magnesium chloride, were all of analytical grade and purchased from Sinopharm Chemical Reagent Co., Ltd.. Deionized water was used to prepare the saline solution.

4.2. Polyacrylamide Synthesis

Polyacrylamide was synthesized in the laboratory, and the preparation process was similar to our previous report [50], with some modifications. In a typical procedure, 30 g of AM monomer was dissolved in 160 mL of water and transferred into a 500 mL three-neck round-bottom flask at 70 °C. Nitrogen gas was purged through the solution for 30 minutes at a flow rate of 50 mL/min to remove dissolved oxygen. Subsequently, 60 mg of $K_2S_2O_8$ was dissolved in 10 mL of water and added dropwise to the flask to initiate polymerization. The solution was continuously stirred under nitrogen and heated at 70 °C for 4.5 hours. Then, 400 mL of water was gradually added to dilute the polymer solution, resulting in a uniform polymer stock liquor with a concentration of 5 wt%. The viscosity-average molecular weight of the synthesized PAM was measured to be 1.40×10^6 using an Ubbelohde viscometer. The degree of hydrolysis was determined to be 1.3% through titration.

4.3. Gel sample Preparation

Sodium chloride, calcium chloride, and magnesium chloride were used to prepare a brine stock solution with a total dissolved solids of 30×10^4 mg/L, utilizing deionized water. After dilution, brine solutions with different mineralization levels were produced to simulate formation water. The composition of the brine stock solution is outlined in Table 7.

Table 7. Composition of brine stock solution.

ion concentration/mg·L^{-1}				total dissolved solids/mg·L^{-1}
Na^+	Ca^{2+}	Mg^{2+}	Cl^-	
99,998.7	6,816.0	6,818.6	186,366.7	3.0×10^5

 doi:10.20944/preprints202502.1604.v1

In preparing the gel reaction solution, the polymer, brine stock solutions, and deionized water were combined in specified proportions to ensure that the sample's salinity ranged from 5 to 20×10^4 mg/L, while the polyacrylamide concentration was maintained between 0.5-2.0 wt%. Crosslinking agents, including formaldehyde (0.15-0.40 wt%), HQ (0.16-0.42 wt%), and thiourea stabilizer (0.05 wt%), were subsequently incorporated. Urea was then added and mixed thoroughly, resulting in a gel reaction solution, commonly referred to as gelant.

4.4. Structure Characterization and Morphology Observation

The polymer samples and freshwater gel samples were freeze-dried separately and then crushed. They were subsequently mixed with KBr and ground at a mass ratio of 1:100 (polymer to KBr) before being pressed into pellets. The resulting samples were analyzed using a Bruker Vertex 70 Fourier Transform Infrared Spectrometer over a wavenumber range of 400 to 4000 cm^{-1}.

To analyze the structure of the inorganic components in the composite gel, a brine solution with a mineralization degree of 15×10^4 mg/L was used. Urea was added in an amount equivalent to that of the composite gel with N=1, excluding polymers and crosslinking agents. The sample was heated at 95 °C for 30 days to ensure adequate precipitation. Following washing with water, drying, and grinding, X-ray diffraction (XRD) analysis was conducted using a Japan Rigaku X-ray diffractometer (D/MAX-2500/PC) equipped with a Cu Kα radiation source (40 kV, 150 mA, λ=1.54051 Å) to examine the crystalline structure of the inorganic components. The analysis was performed over a diffraction angle range of 2θ = 5-70 °, with a scanning speed of 10 °/min.

The morphology of the samples was examined using a field emission scanning electron microscope (JSM-6700F) from JEOL, facilitating a comparative analysis of the morphological characteristics of BG and CG. Due to the significant presence of inorganic salts in both BG and CG samples, inorganic salt particles precipitated from the liquid phase and adhered to the surface of the polymer during the direct observation of the gel samples. Consequently, this study also included washing the BG and CG samples with water to remove soluble inorganic salts. Afterward, the samples were freeze-dried and coated with gold for surface treatment, allowing for morphological observations to compare and analyze the characteristics of the BG and CG samples before and after washing.

4.5. Gelation Performance Observation

The evaluation of gel strength, gelation time, and stability time was conducted following the Gel Strength Codes (GSC) method as proposed by Sydansk et al. [8,47–49]. The procedure involved sealing 20 mL of gelant in an ampoule and placing it in a temperature-controlled oven for heating. The gel strength was observed and the corresponding code was recorded at certain time.

4.6. Rheological Testing

Dynamic rheological performance tests of FG, BG, and CG were conducted using a parallel plate rotational rheometer (ARES-G2) from TA Instruments, USA. The primary focus was on the measurement of the elastic modulus (G′) and viscous modulus (G′′), as well as the influence of factors such as urea concentration and salinity on the strength of the composite gel. During the experiment, the oscillation frequency was initially set at 1 Hz (6.28 rad/s) for strain scanning to identify the linear viscoelastic region of the sample, where the complex modulus remains constant with shear stress. Following this, frequency scanning was carried out within the established linear viscoelastic region, with oscillation frequencies ranging from 0.01 to 10 Hz, to determine G′ and G′′, while maintaining the experimental temperature at 25 °C.

4.7. Thermal Stability Testing

Thermogravimetric and differential scanning calorimetry (TG-DSC) analyses of the FG, BG, and CG samples were performed using a PerkinElmer STA 8000 thermal analyzer to assess the thermal

 doi:10.20944/preprints202502.1604.v1

stability of the dried gel samples. During the experiment, the samples were heated in a nitrogen atmosphere at a rate of 10 °C/min, with the temperature range set between 30 and 900 °C.

Author Contributions: Conceptualization, D.L. and J.Z.; methodology, J.Z.; software, L.L.; validation, L.L. and J.L.; formal analysis, L.L.; investigation, L.L. and J.L.; resources, D.L.; data curation, L.L. and J.Z.; writing—original draft preparation, L.L.; writing—review and editing, J.Z.; visualization, J.X.; supervision, B.Z.; project administration, J.Z.; funding acquisition, D.L. All authors have read and agreed to the published version of the manuscript.

Funding: This research was funded by the National Natural Science Foundation of China (No. 21975139), the Natural Science Foundation of Shandong Province (No. ZR2017MB042), China.

Institutional Review Board Statement: Not applicable.

Informed Consent Statement: Not applicable.

Data Availability Statement: The data that support findings of this study are available from the corresponding authors upon reasonable request.

Conflicts of Interest: The authors declare no conflicts of interest.

References

1. Moradi-Araghi, A. A review of thermally stable gels for fluid diversion in petroleum production. *J. Pet. Sci. Eng.* **2000**, *26*, 1-10. https://doi.org/10.1016/S0920-4105(00)00015-2.
2. Naficy, S.; Brown, H.R.; Razal, J.M.; Spinks, G.M.; Whitten, P.G. Progress toward robust polymer hydrogels. *Aust. J. Chem.* **2011**, *64*, 1007-1025. https://doi.org/10.1071/CH11156.
3. Bai, B.; Zhou, J.; Yin, M. A comprehensive review of polyacrylamide polymer gels for conformance control. *Pet. Explor. Develop.* **2015**, *42*, 525-532. https://doi.org/10.1016/S1876-3804(15)30045-8.
4. Zhu, D.; Bai, B.; Hou, J. Polymer gel systems for water management in high-temperature petroleum reservoirs: A chemical review. *Energy Fuels* **2017**, *31*, 13063-13087. https://doi.org/10.1021/acs.energyfuels.7b02897.
5. Amir, Z.; Said, I.M.; Jan, B.M. In situ organically cross-linked polymer gel for high-temperature reservoir conformance control: A review. *Polym. Adv. Technol.* **2018**, *30*, 13-39. https://doi.org/10.1002/pat.4455.
6. Kang, W.; Kang, X.; Lashari, Z.A.; Li, Z.; Zhou, B.; Yang, H.; et al. Progress of polymer gels for conformance control in oilfield. *Adv. Colloid Interface Sci.* **2021**, *289*, 102363. https://doi.org/10.1016/j.cis.2021.102363.
7. Guzmán-Lucero, D.; Martínez-Palou, R.; Palomeque-Santiago, J.F.; Vega-Paz, A.; Guzmán-Pantoja, J.; López-Falcón, D.A.; et al. Water control with gels based on synthetic polymers under extreme conditions in oil wells. *Chem. Eng. Technol.* **2022**, *45*, 998-1016. https://doi.org/10.1002/ceat.202100648.
8. Zhang, G.; Chen, L.; Ge, J.; Jiang, P.; Zhu, X. Experimental research of syneresis mechanism of HPAM/Cr^{3+} gel. *Colloids Surf. A Physicochem. Eng. Asp.* **2015**, *483*, 96-103. https://doi.org/10.1016/j.colsurfa.2015.07.048.
9. Xiong, C.; Wei, F.; Li, W.; Liu, P.; Wu, Y.; Dai, M.; et al. Mechanism of polyacrylamide hydrogel instability on high-temperature conditions. *ACS Omega* **2018**, *3*, 10716-10724. https://doi.org/10.1021/acsomega.8b01205.
10. Sengupta, B.; Sharma, V.P.; Udayabhanu, G. Gelation studies of an organically cross-linked polyacrylamide water shut-off gel system at different temperatures and pH. *J. Pet. Sci. Eng.* **2012**, *81*, 145-150. https://doi.org/10.1016/j.petrol.2011.12.016.
11. Xu, Z.; Zhao, M.; Sun, N.; Meng, X.; Yang, Z.; Xie, Y.; et al. Delayed crosslinking gel fracturing fluid with dually crosslinked polymer network for ultra-deep reservoir: Performance and delayed crosslinking mechanism [J]. *Colloids Surf. A Physicochem. Eng. Asp.* **2025**, *708*, 135967. https://doi.org/10.1016/j.colsurfa.2024.135967.
12. Fang, J.; Zhang, X.; He, L.; Zhao, G.; Dai, C. Experimental research of hydroquinone (HQ)/hexamethylene tetramine (HMTA) gel for water plugging treatments in high-temperature and high-salinity reservoirs. *J. Appl. Polym. Sci.* **2016**, *134*, 43359. https://doi.org/10.1002/app.44359.

 doi:10.20944/preprints202502.1604.v1

13. Liu, Y.; Dai, C.; Wang, K.; Zhao, M.; Zhao, G.; Yang, S.; et al. New insights into the hydroquinone (HQ)-hexamethylenetetramine (HMTA) gel system for water shut-off treatment in high temperature reservoirs. *J. Ind. Eng. Chem.* **2016**, *35*, 20-28. https://doi.org/10.1016/j.jiec.2015.09.032.
14. Zhu, D.; Hou, J.; Wei, Q.; Wu, X.; Bai, B. Terpolymer gel system formed by resorcinol-hexamethylenetetramine for water management in extremely high-temperature reservoirs. *Energy Fuels* **2017**, *31*, 1519-1528. https://doi.org/10.1021/acs.energyfuels.6b03188.
15. Bryant, S.L.; Bartosek, M.; Lockhart, T.P. Laboratory evaluation of phenol-formaldehyde/polymer gelants for high-temperature applications. *J. Pet. Sci. Eng.* **1997**, *17*, 197-209. https://doi.org/10.1016/S0920-4105(96)00079-4.
16. Li, Q.; Yu, X.; Wang, L.; Qu, S.; Wu, W.; Ji, R.; et al. Nano-silica hybrid polyacrylamide/polyethylenimine gel for enhanced oil recovery at harsh conditions. *Colloids Surf. A Physicochem. Eng. Asp.* **2022**, *633*, 127898. https://doi.org/10.1016/j.colsurfa.2021.127898.
17. Tongwa, P.; Nygaard, R.; Bai, B. Evaluation of a nanocomposite hydrogel for water shut-off in enhanced oil recovery applications: design, synthesis, and characterization. *J. Appl. Polym. Sci.* **2012**, *128*, 787-794. https://doi.org/10.1002/app.38258.
18. Michael, F.M.; Fathima, A.; AlYemni, E.; Jin, H.; Almohsin, A.; Alsharaeh, E.H. Enhanced polyacrylamide polymer gels using zirconium hydroxide nanoparticles for water shutoff at high temperatures: Thermal and rheological investigations. *Ind. Eng. Chem. Res.* **2018**, *57*, 16347-16357. https://doi.org/10.1021/acs.iecr.8b04126.
19. Chen, L.; Wang, J.; Yu, L.; Zhang, Q.; Fu, M.; Zhao, Z.; et al. Experimental investigation on the nanosilica-reinforcing polyacrylamide/polyethylenimine hydrogel for water shutoff treatment. *Energy Fuels* **2018**, *32*, 6650-6656. https://doi.org/10.1021/acs.energyfuels.8b00840.
20. Azimi Dijvejin, Z.; Ghaffarkhah, A.; Sadeghnejad, S.; Vafaie Sefti, M. Effect of silica nanoparticle size on the mechanical strength and wellbore plugging performance of SPAM/chromium (III) acetate nanocomposite gels. *Polym. J.* **2019**, *51*, 693-707. https://doi.org/10.1038/s41428-019-0178-3.
21. Liu, Y.; Dai, C.; Wang, K.; Zou, C.; Gao, M.; Fang, Y.; et al. Study on a novel cross-linked polymer gel strengthened with silica nanoparticles. *Energy Fuels* **2017**, *31*, 9152-9161. https://doi.org/10.1021/acs.energyfuels.7b01432.
22. Telin, A.; Safarov, F.; Yakubov, R.; Gusarova, E.; Pavlik, A.; Lenchenkova, L.; et al. Thermal degradation study of hydrogel nanocomposites based on polyacrylamide and nanosilica used for conformance control and water shutoff. *Gels* **2024**, *10*, 846. https://doi.org/10.3390/gels10120846.
23. Almeida, A.I.A.D.R.; Carvalho, L.D.O.; Lopes, R.C.F.G.; Sena, L.E.B.; Amparo, S.E.Z.S.D.; Oliveira, C.P.M.D.; et al. Enhanced polyacrylamide polymer hydrogels using nanomaterials for water shutoff: Morphology, thermal and rheological investigations at high temperatures and salinity. *J. Mol. Liq.* **2024**, *405*, 125041. https://doi.org/10.1016/j.molliq.2024.125041.
24. Pérez-Robles, S.; Cortés, F.B.; Franco, C.A. Effect of the nanoparticles in the stability of hydrolyzed polyacrylamide/resorcinol/formaldehyde gel systems for water shut-off/conformance control applications. *J. Appl. Polym. Sci.* **2019**, *136*, 47568. https://doi.org/10.1002/app.47568.
25. Otsuka, T.; Chujo, Y. Poly(methyl methacrylate) (PMMA)-based hybrid materials with reactive zirconium oxide nanocrystals. *Polym. J.* **2010**, *42*, 58-65. https://doi.org/10.1038/pj.2009.309.
26. Adewunmi, A.A.; Ismail, S.; Sultan, A.S. Study on strength and gelation time of polyacrylamide/polyethyleneimine composite gels reinforced with coal fly ash for water shut-off treatment. *J. Appl. Polym. Sci.* **2014**, *132*, 41392. https://doi.org/10.1002/app.41392.
27. Wang, K.; Wang, S.; Wang, X.; Wang, X.; Zheng, L.; Wen, J.; et al. Modulation of syneresis rate and gel strength of PAM-PEI gels by nanosheets and their mechanisms. *Colloids Surf. A Physicochem. Eng. Asp.* **2025**, *704*, 135525. https://doi.org/10.1016/j.colsurfa.2024.135525.
28. Gao, G.; Du, G.; Sun, Y.; Fu, J. Self-healable, tough, and ultrastretchable nanocomposite hydrogels based on reversible polyacrylamide/montmorillonite adsorption. *ACS Appl. Mater. Interfaces* **2015**, *7*, 5029-5037. https://doi.org/10.1021/acsami.5b00704.
29. Helvacıoğlu, E.; Aydın, V.; Nugay, T.; Nugay, N.; Uluocak, B.G.; Şen, S. High strength poly(acrylamide)-clay hydrogels. *J. Polym. Res.* **2011**, *18*, 2341-2350. https://doi.org/10.1007/s10965-011-9647-x.

 doi:10.20944/preprints202502.1604.v1

30. Zolfaghari, R.; Katbab, A.A.; Nabavizadeh, J.; Tabasi, R.Y.; Nejad, M.H. Preparation and characterization of nanocomposite hydrogels based on polyacrylamide for enhanced oil recovery applications. *J. Appl. Polym. Sci.* **2006**, *100*, 2096-2103. https://doi.org/10.1002/app.23193.
31. Pereira, K.A.B.; Aguiar, K.; Oliveira, P.F.; Vicente, B.M.; Pedroni, L.G.; Mansur, C.R.E. Synthesis of hydrogel nanocomposites based on partially hydrolyzed polyacrylamide, polyethyleneimine, and modified clay. *ACS Omega* **2020**, *5*, 4759-4769. https://doi.org/10.1021/acsomega.9b02829.
32. Bai, Y.; Shang, X.; Wang, Z.; Zhao, X. Experimental study of low molecular weight polymer/nanoparticle dispersed gel for water plugging in fractures. *Colloids Surf. A Physicochem. Eng. Asp.* **2018**, *551*, 95-107. https://doi.org/10.1016/j.colsurfa.2018.04.067.
33. Fu, P.; Xu, K.; Song, H.; Chen, G.; Yang, J.; Niu, Y. Preparation, stability and rheology of polyacrylamide/pristine layered double hydroxide nanocomposites. *J. Mater. Chem.* **2010**, *20*, 3869-3876. https://doi.org/10.1039/B927391C.
34. Zhang, H.-P.; Cao, J.-J.; Jiang, W.-B.; Yang, Y.-Q.; Zhu, B.-Y.; Liu, X.-Y.; et al. Synthesis and mechanical properties of polyacrylamide gel doped with graphene oxide. *Energies* **2022**, *15*, 5714. https://doi.org/10.3390/en15155714.
35. Shi, B.; Zhang, G.; Zhang, L.; Wang, C.; Li, Z.; Chen, F. Study on a strong polymer gel by the addition of micron graphite oxide powder and its plugging of fracture. *Gels* **2024**, *10*, 304. https://doi.org/10.3390/gels10050304.
36. Moradi-Araghi, A.; Doe, P.H. Hydrolysis and precipitation of polyacrylamides in hard brines at elevated temperatures. *SPE Reservoir Eng.* **1987**, *2*, 189-198. https://doi.org/10.2118/13033-PA.
37. Ma, Q.; Shuler, P.J.; Aften, C.W.; Tang, Y. Theoretical studies of hydrolysis and stability of polyacrylamide polymers. *Polym. Degrad. Stab.* **2015**, *121*, 69-77. https://doi.org/10.1016/j.polymdegradstab.2015.08.012.
38. Marandi, G.B.; Esfandiari, K.; Biranvand, F.; Babapour, M.; Sadeh, S.; Mahdavinia, G.R. pH sensitivity and swelling behavior of partially hydrolyzed formaldehyde-crosslinked poly(acrylamide) superabsorbent hydrogels. *J. Appl. Polym. Sci.* **2008**, *109*, 1083-1092. https://doi.org/10.1002/app.28205.
39. Fong, D.W.; Kowalski, D.J. An investigation of the crosslinking of polyacrylamide with formaldehyde using 13C nuclear magnetic resonance spectroscopy. *J. Polym. Sci., Part A: Polym. Chem.* **1993**, *31*, 1625-1627. https://doi.org/10.1002/pola.1993.080310633.
40. Cheng, L.; Qin, Y.; Su, Y.; Pan, Y.; Wang, Y.; Liao, R.; et al. Development of a high-strength and adhesive polyacrylamide gel for well plugging. *ACS Omega* **2022**, *7*, 6151-6159. https://doi.org/10.1021/acsomega.1c06626.
41. Ma, Z.; Zhao, M.; Yang, Z.; Wang, X.; Dai, C. Development and gelation mechanism of ultra-high-temperature-resistant polymer gel. *Gels* **2023**, *9*, 726. https://doi.org/10.3390/gels9090726.
42. Zhu, D.; Hou, J.; Meng, X.; Zheng, Z.; Wei, Q.; Chen, Y.; et al. Effect of different phenolic compounds on performance of organically cross-linked terpolymer gel systems at extremely high temperatures. *Energy Fuels* **2017**, *31*, 8120-8130. https://doi.org/10.1021/acs.energyfuels.7b01386.
43. Reddy, B.R.; Eoff, L.; Dalrymple, E.D.; Black, K.; Brown, D.; Rietjens, M. A natural polymer-based crosslinker system for conformance gel systems. *SPE J.* **2003**, *8*, 99-106. https://doi.org/10.2118/84937-PA.
44. Li, Z.-Y.; Li, X.-G.; Du, K.; Liu, H.-K. Development of a new high-temperature and high-strength polymer gel for plugging fractured reservoirs. *Upstream Oil Gas Technol.* **2020**, *5*, 100014. https://doi.org/10.1016/j.upstre.2020.100014.
45. Fox, K.B.; Evans, A.Jr. Acceleration of gelation of water soluble polymers. United States patent US 5447986, 5 Sep 1995.
46. Ren, Q.; Jia, H.; Yu, D.; Pu, W.-F.; Wang, L.-L.; Li, B.; et al. New insights into phenol-formaldehyde-based gel systems with ammonium salt for low-temperature reservoirs. *J. Appl. Polym. Sci.* **2014**, *131*, 40657. https://doi.org/10.1002/app.40657.
47. Hakiki, F.; Arifurrahman, F. Cross-linked and responsive polymer: gelation model and review. *J. Ind. Eng. Chem.* **2023**, *119*, 532-549. https://doi.org/10.1016/j.jiec.2022.11.076.
48. Xu, P.; Shang, Z.; Yao, M.; Li, X. Mechanistic insight into improving strength and stability of hydrogels via nano-silica. *J. Mol. Liq.* **2022**, *357*, 119094. https://doi.org/10.1016/j.molliq.2022.119094.

 doi:10.20944/preprints202502.1604.v1

49. Zhu, D.; Hou, J.; Chen, Y.; Wei, Q.; Zhao, S.; Bai, B. Evaluation of terpolymer-gel systems crosslinked by polyethylenimine for conformance improvement in high-temperature reservoirs. *SPE J.* **2019**, *24*, 1726-1740. https://doi.org/10.2118/194004-pa.
50. Li, Y.; Wei, Q.; Wang, R.; Zhao, J.; Quan, Z.; Zhan, T.; et al. 3D hierarchical porous nitrogen-doped carbon/Ni@NiO nanocomposites self-templated by cross-linked polyacrylamide gel for high performance supercapacitor electrode. *J. Colloid Interface Sci.* **2020**, *570*, 286-299. https://doi.org/10.1016/j.jcis.2020.03.004.
51. Lu, G.; Zhao, J.; Li, S.; Chen, Y.; Li, C.; Wang, Y.; et al. Incorporation of partially hydrolyzed polyacrylamide with zwitterionic units and poly(ethylene glycol) units toward enhanced tolerances to high salinity and high temperature. *Front. Mater.* **2021**, *8*, 788746. https://doi.org/10.3389/fmats.2021.788746.
52. Yang, H.; Yan, R.; Chen, H.; Lee, D.H.; Zheng, C. Characteristics of hemicellulose, cellulose and lignin pyrolysis. *Fuel* **2007**, *86*, 1781-1788. https://doi.org/10.1016/j.fuel.2006.12.013.
53. Wang, C. Control the polymorphism and morphology of calcium carbonate precipitation from a calcium acetate and urea solution. *Mater. Lett.* **2008**, *62*, 2377-2380. https://doi.org/10.1016/j.matlet.2007.12.020.
54. De Silva, P.; Bucea, L.; Sirivivatnanon, V. Chemical, microstructural and strength development of calcium and magnesium carbonate binders. *Cem. Concr. Res.* **2009**, *39*, 460-465. https://doi.org/10.1016/j.cemconres.2009.02.003.
55. Douglas, T.E.L.; Łapa, A.; Samal, S.K.; Declercq, H.A.; Schaubroeck, D.; Mendes, A.C.; et al. Enzymatic, urease-mediated mineralization of gellan gum hydrogel with calcium carbonate, magnesium-enriched calcium carbonate and magnesium carbonate for bone regeneration applications. *J. Tissue Eng. Regener. Med.* **2017**, *11*, 3556-3566. https://doi.org/10.1002/term.2273.
56. Krajewska, B. Urease-aided calcium carbonate mineralization for engineering applications: A review. *J. Adv. Res.* **2018**, *13*, 59-67. https://doi.org/10.1016/j.jare.2017.10.009.
57. Wu, Y.; Ajo-Franklin, J.B.; Spycher, N.; Hubbard, S.S.; Zhang, G.; Williams, K.H.; et al. Geophysical monitoring and reactive transport modeling of ureolytically-driven calcium carbonate precipitation. *Geochem. Trans.* **2011**, *12*, 7. https://doi.org/10.1186/1467-4866-12-7.
58. Digiacomo, P.M.; Schramm, C.M. Mechanism of polyacrylamide gel syneresis determined by C-13 NMR. Paper SPE 11787, International Symposium on Oilfield and Geothermal Chemistry, Denver, USA, June 1-3; Society of Petroleum Engineers: Texas, USA, 1983. https://doi.org/10.2118/11787-MS.
59. Rauner, N.; Meuris, M.; Dech, S.; Godde, J.; Tiller, J.C. Urease-induced calcification of segmented polymer hydrogels-A step towards artificial biomineralization. *Acta. Biomater.* **2014**, *10*, 3942-3951. https://doi.org/10.1016/j.actbio.2014.05.021.
60. Albonico, P.; Lockhart, T.P. Divalent ion-resistant polymer gels for high-temperature applications: Syneresis Inhibiting Additives. Paper SPE 25220, SPE International Symposium on Oilfield Chemistry, New Orleans, USA, March 2-5; Society of Petroleum Engineers: Texas, USA,1993. https://doi.org/10.2118/25220-MS.
61. Gu, C.; Lv, Y.; Fan, X.; Zhao, C.; Dai, C.; Zhao, G. Study on rheology and microstructure of phenolic resin crosslinked nonionic polyacrylamide (NPAM) gel for profile control and water shutoff treatments. *J. Pet. Sci. Eng.* **2018**, *169*, 546-552. https://doi.org/10.1016/j.petrol.2018.06.016.
62. Caulfield, M.J.; Qiao, G.G.; Solomon, D.H. Some aspects of the properties and degradation of polyacrylamides. *Chem. Rev.* **2002**, *102*, 3067-3084. https://doi.org/10.1021/cr010439p.
63. Burrows, H.D.; Ellis, H.A.; Utah, S.I. Adsorbed metal ions as stabilizers for the thermal degradation of polyacrylamide. *Polymer* **1981**, *22*, 1740-1744. https://doi.org/10.1016/0032-3861(81)90397-9.
64. Yang, M.-H. The Two-stages thermal degradation of polyacrylamide. *Polym. Test* **1998**, *17*, 191-198. https://doi.org/10.1016/S0142-9418(97)00036-6.
65. Lee, K.E.; Khan, I.; Morad, N.; Teng, T.T.; Poh, B.T. Thermal behavior and morphological properties of novel magnesium salt–polyacrylamide composite polymers. *Polym. Compos.* **2011**, *32*, 1515-1522. https://doi.org/10.1002/pc.21180.
66. Bhattacharjya, D.; Selvamani, T.; Mukhopadhyay, I. Thermal decomposition of hydromagnesite effect of morphology on the kinetic parameters. *J. Therm. Anal. Calorim.* **2012**, *107*, 439-445. https://doi.org/10.1007/s10973-011-1656-9.

 doi:10.20944/preprints202502.1604.v1